

Shapes analysis for time series

Thibaut Germain*, Samuel Gruffaz, Charles Truong, Alain Durmus, & Laurent Oudre



Objective:

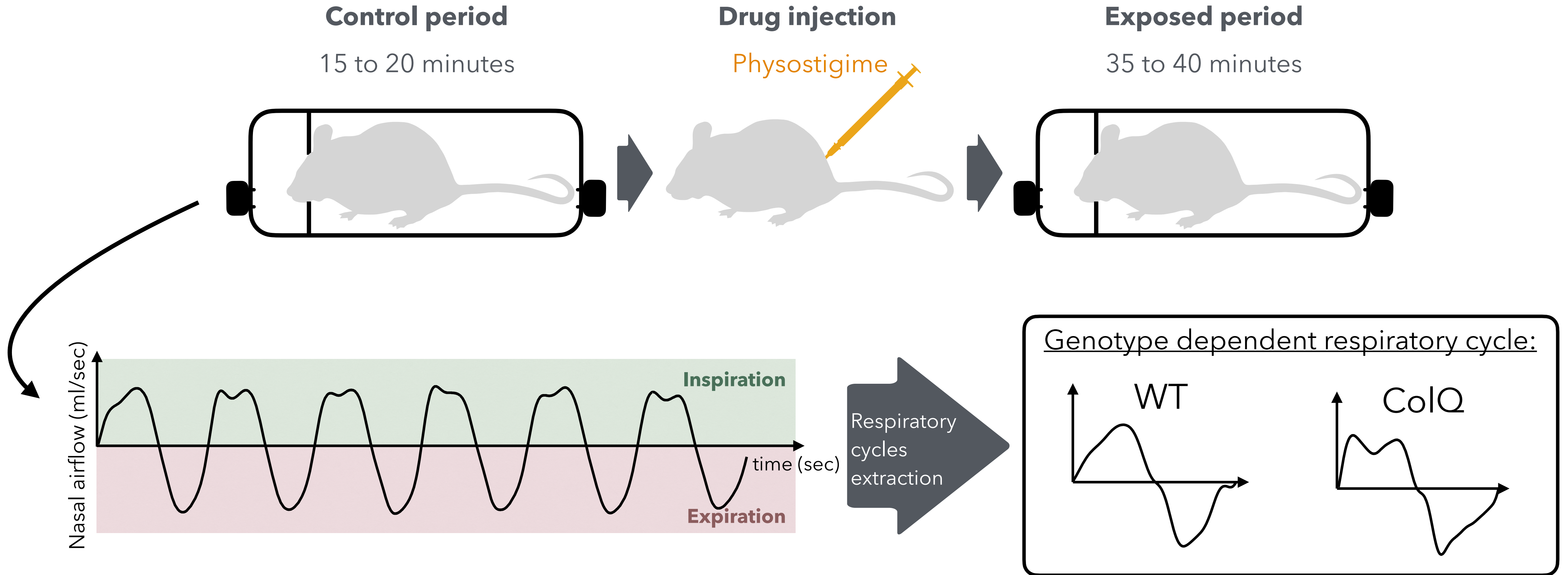
This study aims to analyze **inter-individual variability** within a time series dataset characterized by **irregular sampling** intervals and **variable sequence lengths**.

Methodology:

Unsupervised representation learning with an emphasis on capturing **shape structure**.

An example: mice ventilation analysis

The following experiment was performed for mice of different genotypes (ColQ or WT).



Methodology

Input : $(s_j : I_j \mapsto \mathbb{R}^d)_{j \in [N]}$

1. The shape of s_j is $G_j = \{(t, s_j(t)) : t \in I_j\}$
2. G_j is represented as the deformation of a reference graph $G_0 = \{(t, s_0(t)) : t \in I\}$, i.e. :

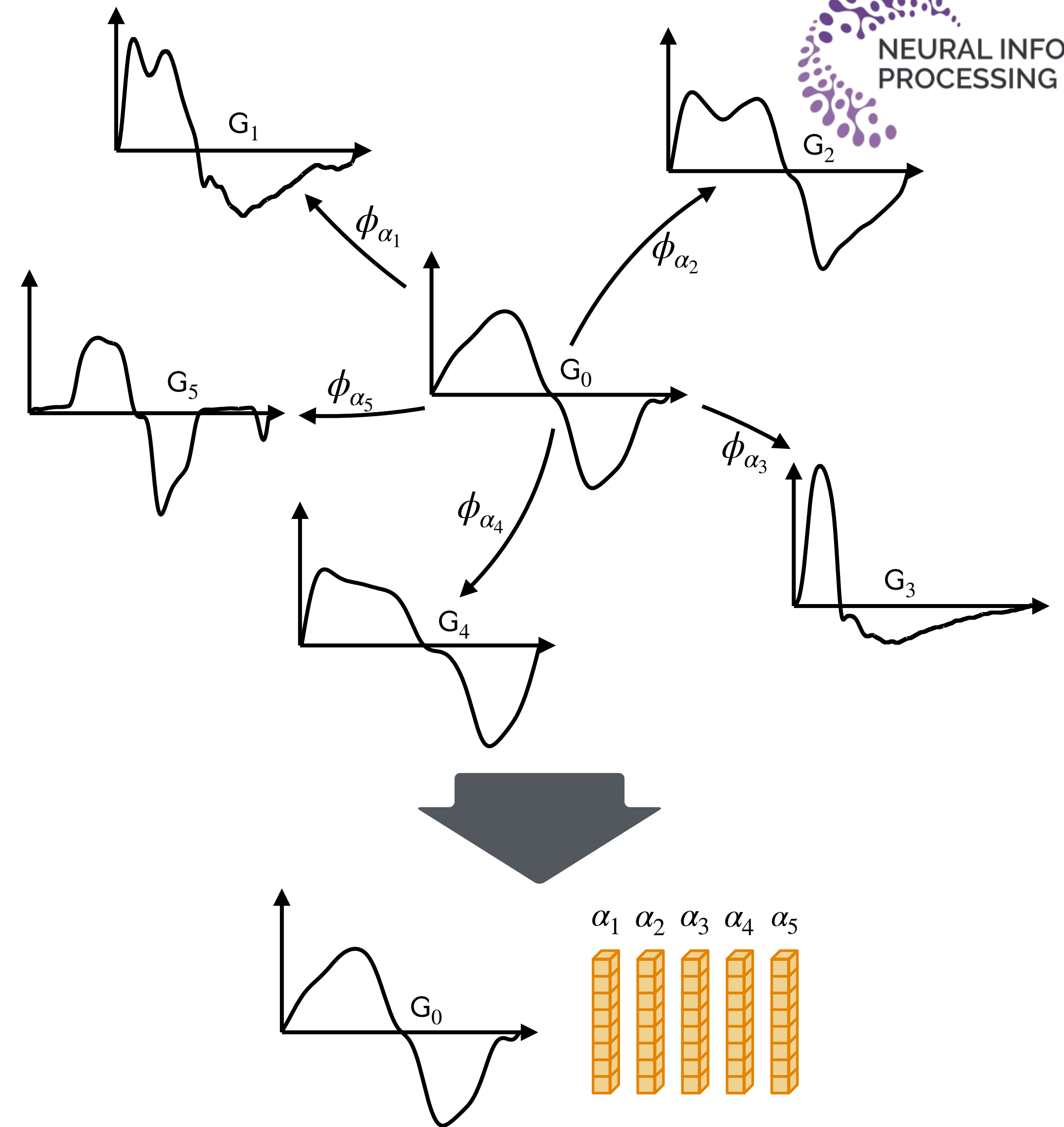
$$G_j \approx \phi_{\alpha_j} \cdot G_0 = \{\phi_{\alpha_j}(t, s_0(t)) : t \in I\},$$

where $\phi_{\alpha_j} : \mathbb{R}^{d+1} \mapsto \mathbb{R}^{d+1}$ is a diffeomorphism parametrized by $\alpha_j \in \mathbb{R}^m$.

3. Learned by solving the empirical Fréchet mean:

$$\arg \min_{G_0, (\alpha_j)_{j \in [N]}} \frac{1}{N} \sum_{j \in [N]} \left(d_G^2(\phi_{\alpha_j} \cdot G_0, G_j) + \lambda d_{\Phi}^2(Id, \phi_{\alpha_j}) \right)$$

Output : a graph of reference $G_0 \subset \mathbb{R}^{d+1}$, deformation parameters $(\alpha_j)_{j \in [N]} \in (\mathbb{R}^m)^N$



Overview

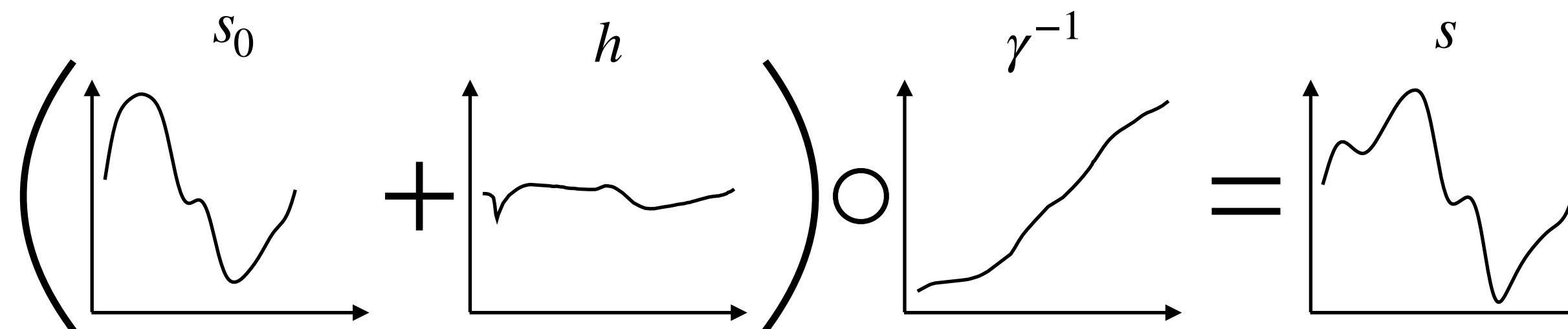
The optimisation problem.

Solved by gradient descent:

$$\arg \min_{\mathbf{G}_0, (\alpha_j)_{j \in [N]}} \frac{1}{N} \sum_{j \in [N]} \left(\underbrace{d_{\mathbf{G}}^2(\phi_{\alpha_j} \cdot \mathbf{G}_0, \mathbf{G}_j)}_{(a)} + \lambda \underbrace{d_{\Phi}^2(\text{Id}, \phi_{\alpha_j})}_{(b)} \right)$$

- (a) Distance measuring the similarity between $\phi_{\alpha_j} \cdot \mathbf{G}_0$ and \mathbf{G}_j embedded as varifold measure [1]. This distance is similar to Maximum Mean Discrepancy (MMD) and is presented in [Section 4.1](#).
- (b) Distance comparing ϕ_{α_j} and Id to privilege minimal diffeomorphic deformation and prevent overfitting. Presented in [Section 3](#).

Deformation requirements. Diffeomorphic deformations are built with the LDDMM framework [2], and presented in [Section 3](#). Our contributions, presented in [Section 4](#), impose that for any $s_0 : \mathbf{I} \mapsto \mathbb{R}^d$ and $s : \mathbf{J} \mapsto \mathbb{R}^d$, the diffeomorphism ϕ mapping s_0 to s is the combination of a distortion $h : \mathbf{I} \mapsto \mathbb{R}$ and a time parametrization $\gamma^{-1} : \mathbf{J} \mapsto \mathbf{I}$ such that: $\phi \cdot \mathbf{G}(s_0) = \mathbf{G}((s_0 + h) \circ \gamma^{-1}) = \mathbf{G}(s)$



Key elements from LDDMM [1]

Generating diffeomorphisms. Assuming $v \in L^2([0,1], V)$ a time-varying velocity field in \mathbb{R}^n , where V is an RKHS with some regularity assumptions [1]. For any $x_0 \in \mathbb{R}^n$, the differential system:

$$\frac{dX(\tau)}{d\tau} = v_\tau(X(\tau)) \quad \text{with} \quad X(0) = x_0$$

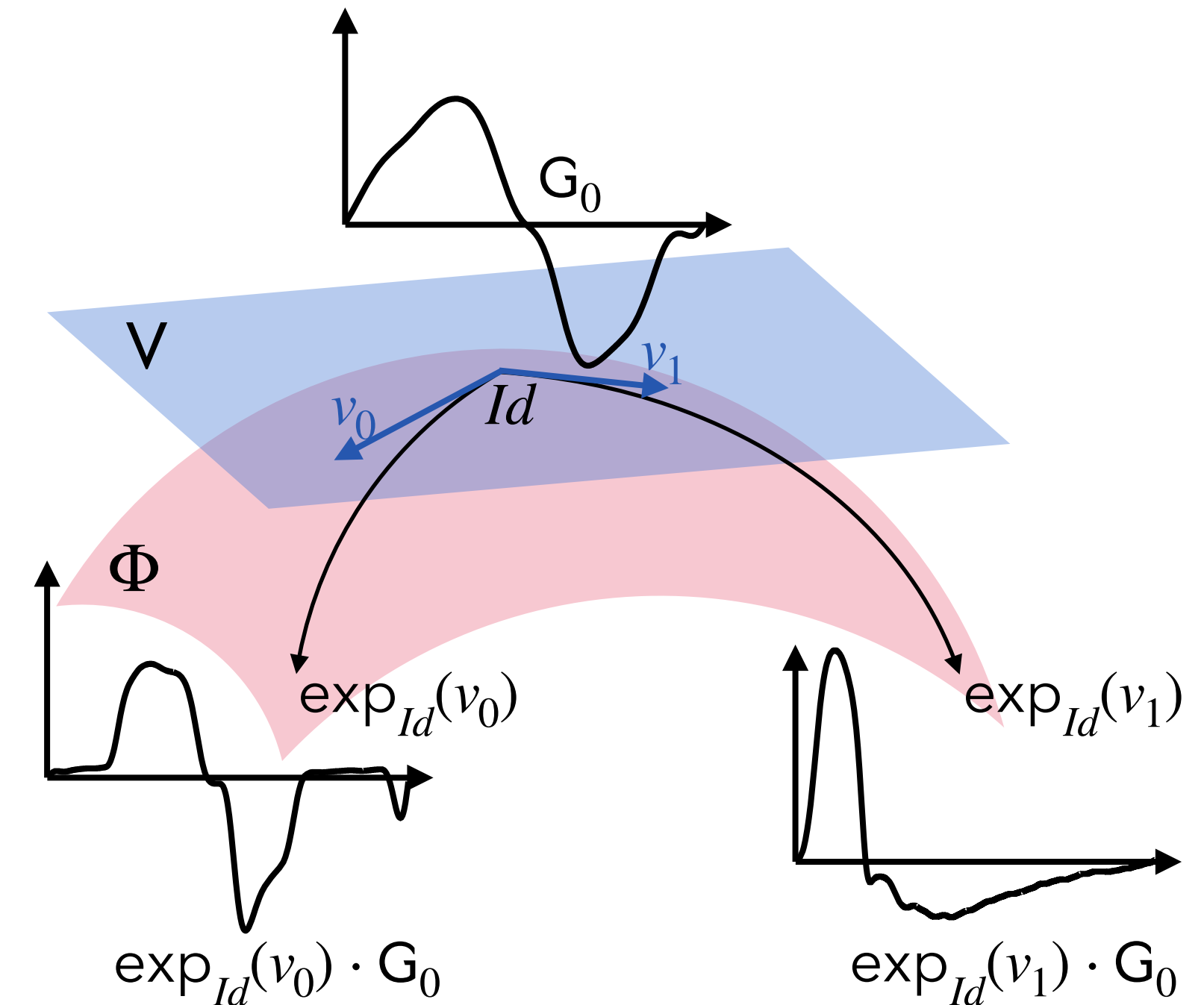
has a unique solution defined for all $\tau \in [0,1]$. The flow application: $\phi_v^\tau : x_0 \in \mathbb{R}^n \mapsto X(\tau) \in \mathbb{R}^n$ solution of (1) at time $\tau \in [0,1]$ is a diffeomorphism. Our interest is in the group of diffeomorphisms: $\Phi \triangleq \{\phi_v^1 \mid v \in L^2([0,1], V)\}$.

Geodesic shooting. Geodesic flow from Id with initial velocity field $v_0 \in V$ can be derived from (2) [2]. By denoting $\tau \mapsto \rho_{v_0}(\tau)$ the geodesic starting from Id with initial conditions $v_0 \in V$, the exponential map is:

$$\exp_{Id} : v_0 \in V \mapsto \rho_{v_0}(1) \in \Phi \quad \text{and} \quad d_\Phi^2(Id, \exp_{Id}(v_0)) = \|v_0\|_V^2$$

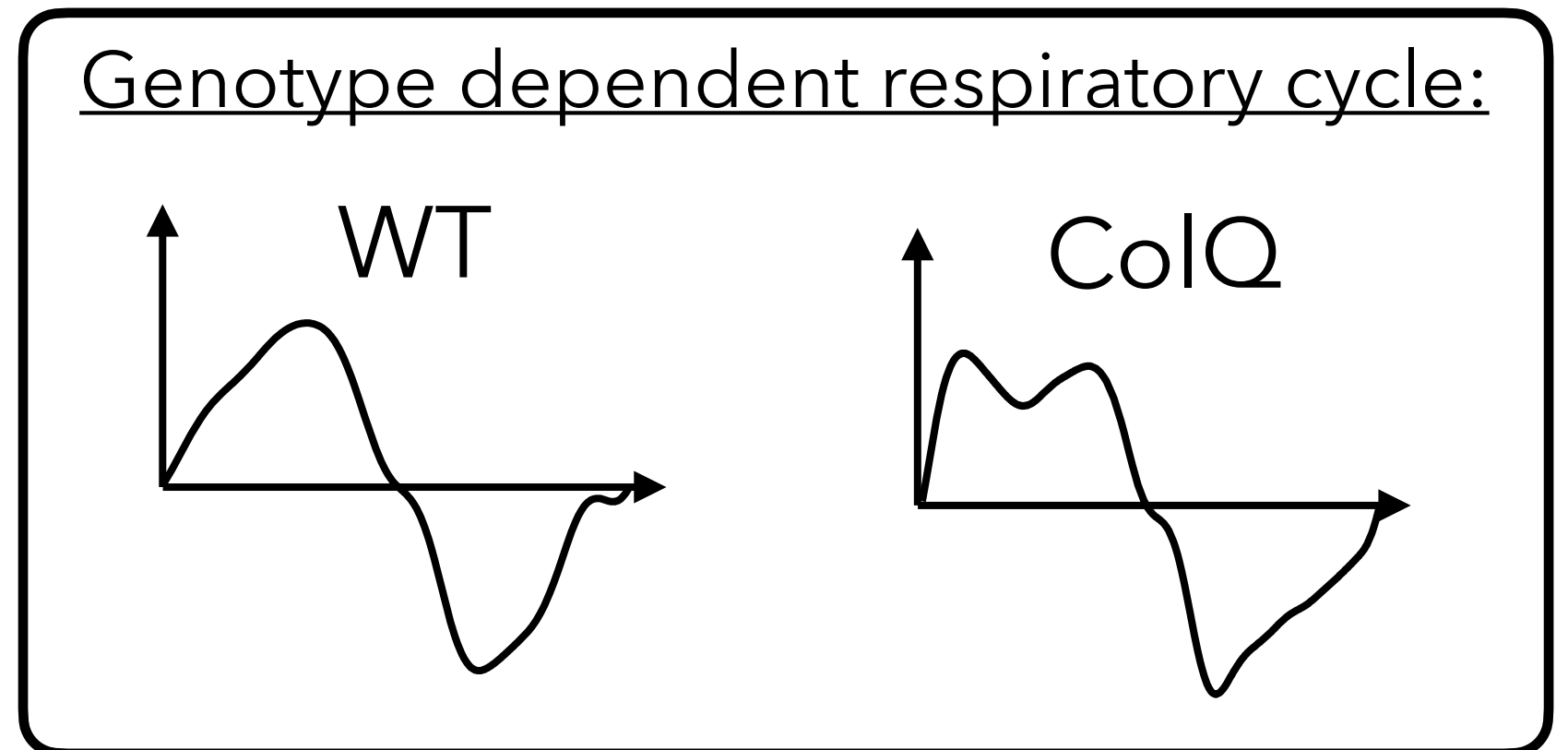
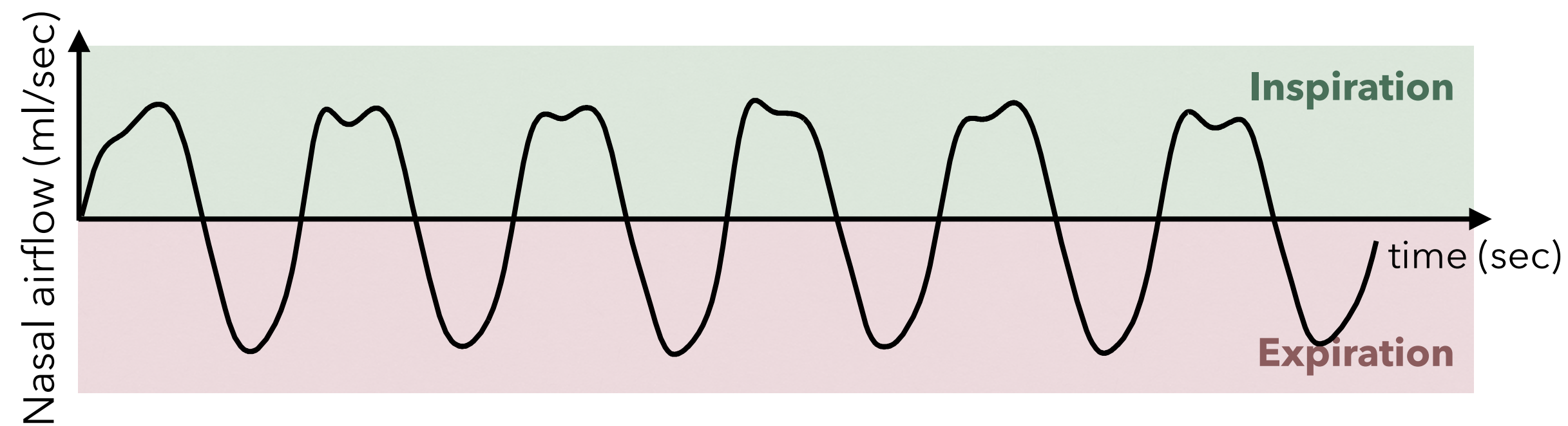
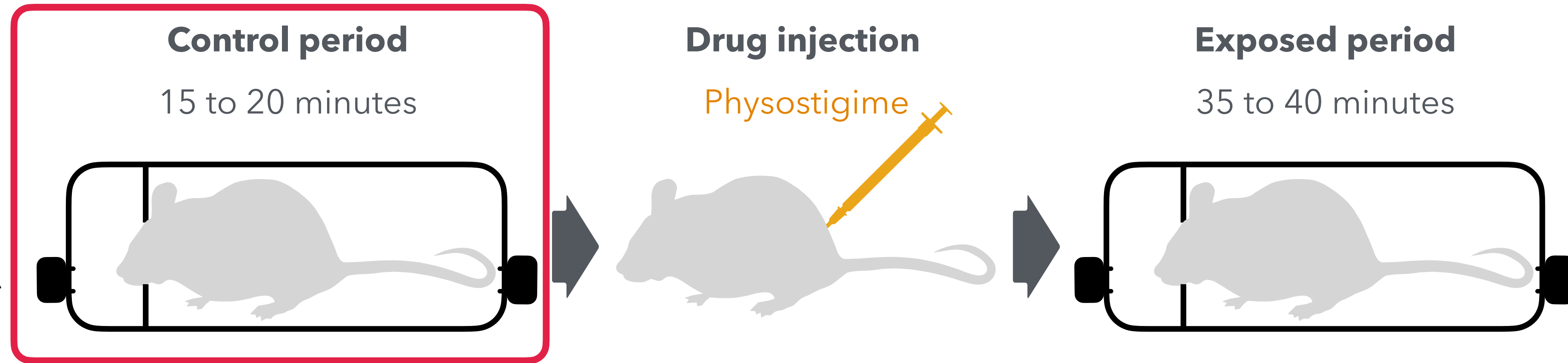
In practice, v_0 is parametrized by K , the kernel associated with V , the sampled time series graph $G_0 \in (\mathbb{R}^{d+1})^{N_0}$ and the parameters $\alpha_0 \in (\mathbb{R}^{d+1})^{N_0}$ such that:

$$v_0 : x \in \mathbb{R}^{d+1} \mapsto \sum_{k \in [N_0]} K(g_0^k, x) \alpha_0^k \in \mathbb{R}^{d+1}$$



An example: mice ventilation analysis before drug injection

For mice of different genotype (ColQ or WT):

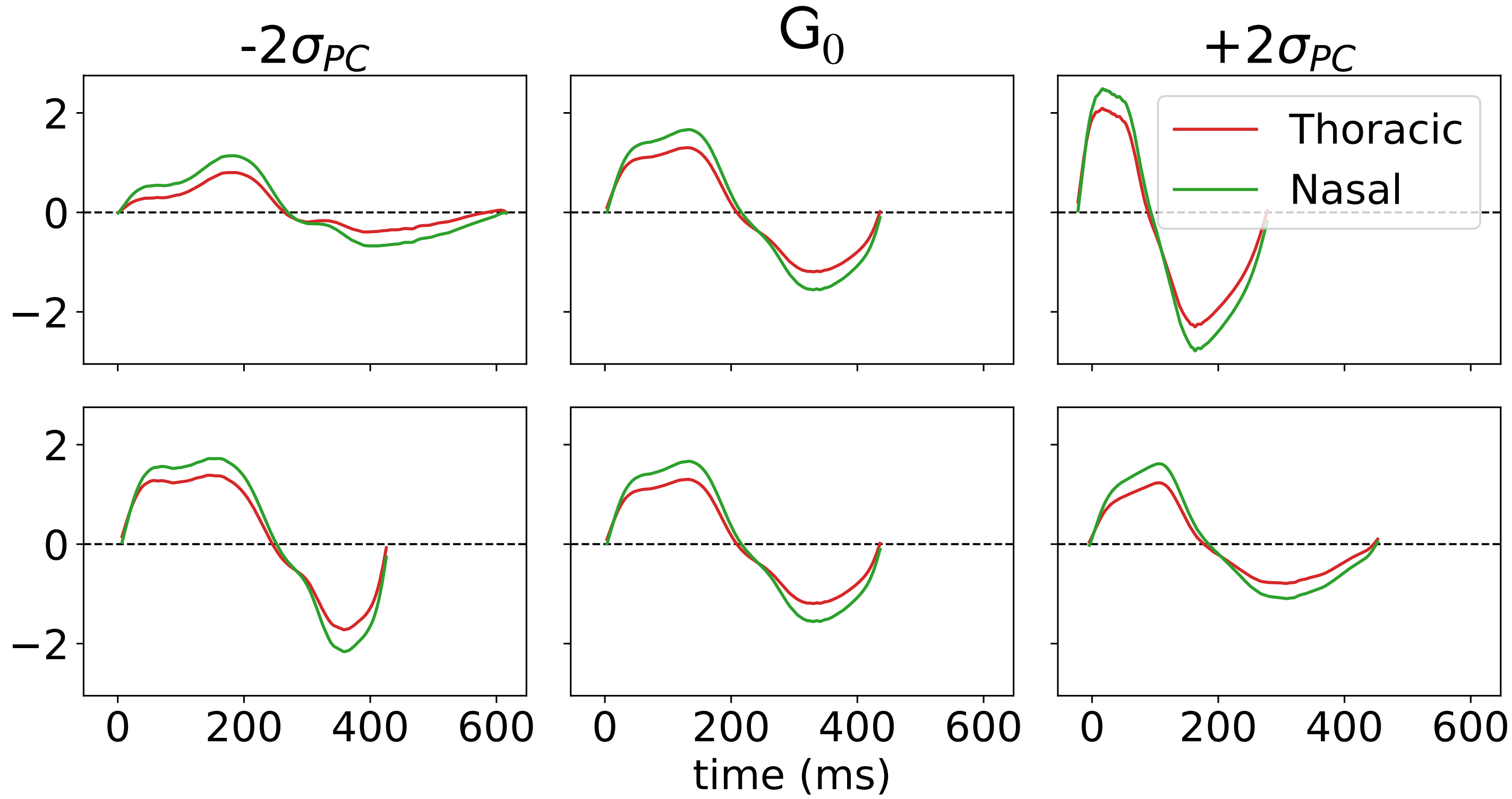
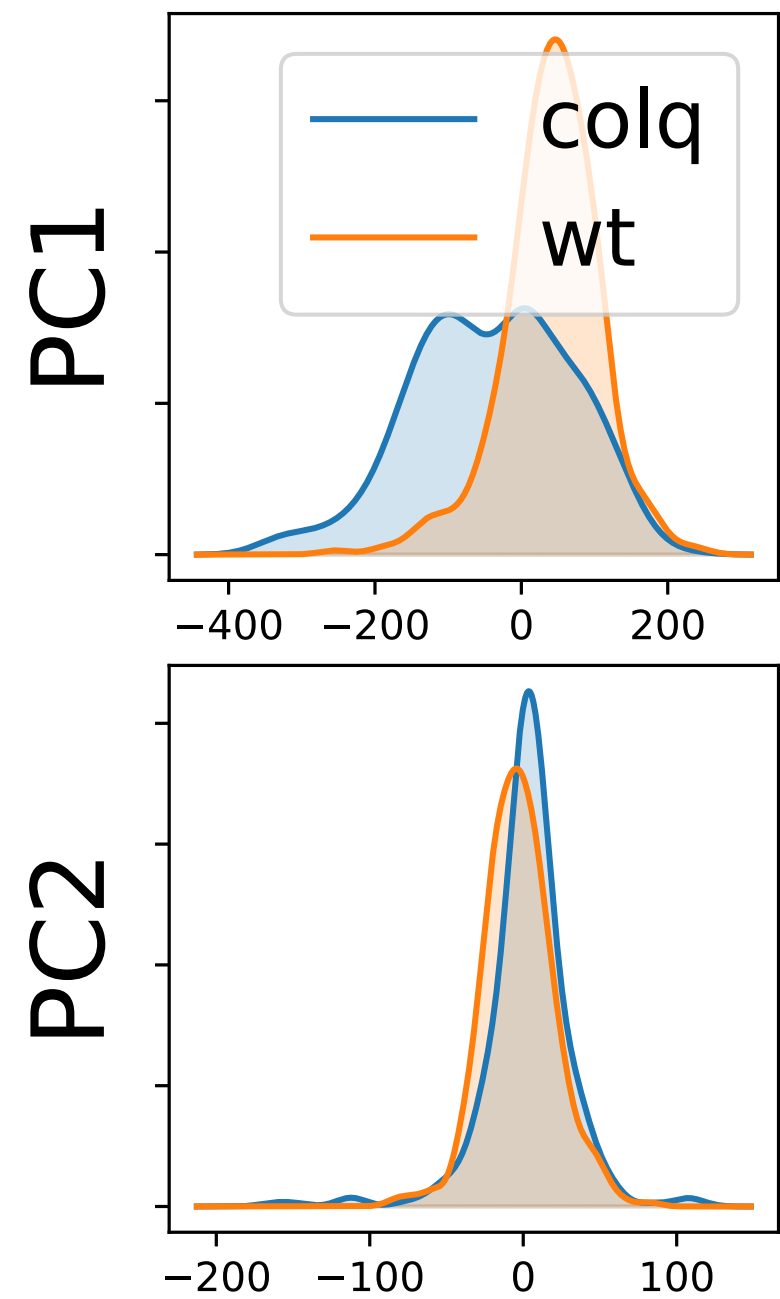


Mice ventilation analysis before drug injection

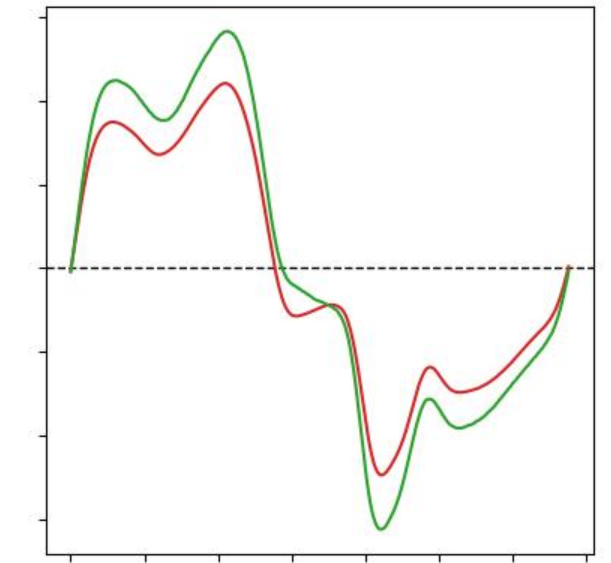
Kernel PCA is applied on the initial velocity field parameters $(\mathbf{G}_0, \alpha_i)_{i \in [N]}$, resulting in the K principal axis of deformations with the initial velocity field $(\mathbf{G}_0, \alpha_j^{PC})_{j \in [K]}$.

Deformations by flowing along PCs:

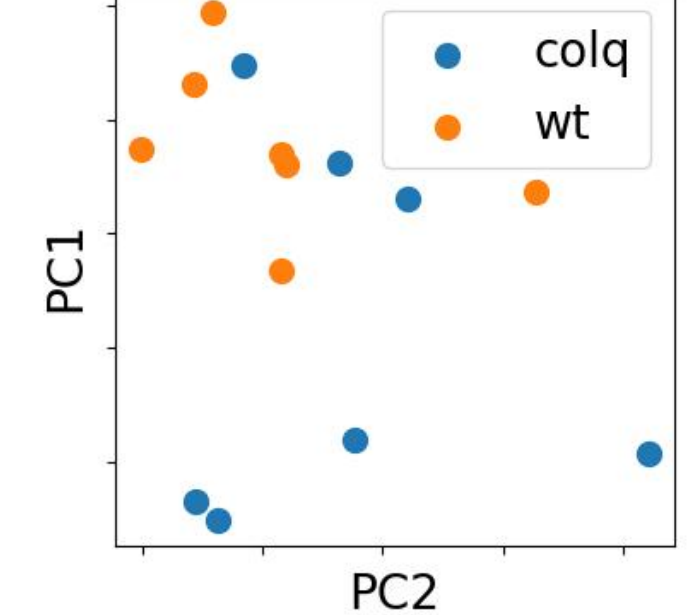
PC densities



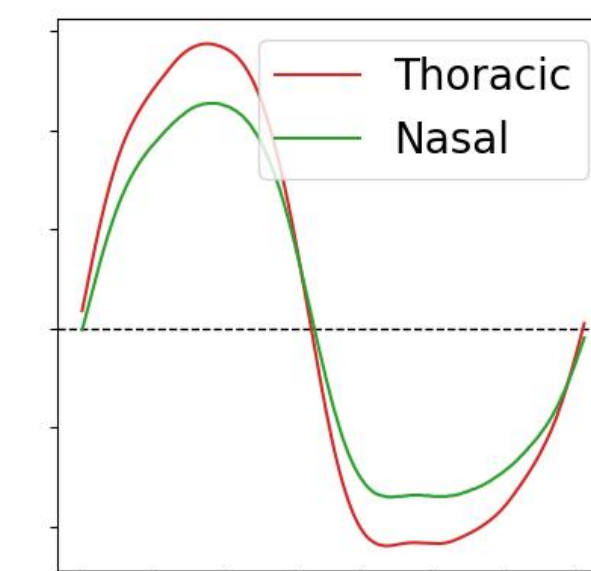
ColQ



PC1/PC2



WT



Thank you !

More details are provided in the next slides

I. Building diffeomorphisms with LDDMM [1]

Generating diffeomorphisms. Assuming $v \in L^2([0,1], V)$ a time-varying velocity field in \mathbb{R}^n , where V is an RKHS with some regularity assumptions [1]. For any $x_0 \in \mathbb{R}^n$, the differential system:

$$\frac{dX(\tau)}{d\tau} = v_\tau(X(\tau)) \quad \text{with} \quad X(0) = x_0, \quad (1)$$

has an unique solution defined for all $\tau \in [0,1]$. The flow application: $\phi_v^\tau : x_0 \in \mathbb{R}^n \mapsto X(\tau) \in \mathbb{R}^n$ solution of (1) at time $\tau \in [0,1]$ is a diffeomorphism.

A metric group. The $\Phi \triangleq \{\phi_v^1 \mid v \in L^2([0,1], V)\}$ is metrizable such that for any $\phi \in \Phi$:

$$d_\Phi^2(Id, \phi) = \inf_{v \in L^2([0,1], V)} \left\{ \int_0^1 \|v_\tau\|_V^2 \mid \phi_v^1 = \phi \right\}, \quad (2)$$

the infimum is reached with a v^* and it conserves its norm along its geodesic path i.e.: $\|v_\tau^*\|_V = \|v_0^*\|_V, \forall \tau \in [0,1]$.

An exponential map. Geodesic flow from Id with initial velocity field $v_0 \in V$ can be derived from (2) [2]. By denoting $\tau \mapsto \rho_{v_0}(\tau)$ the geodesic starting from Id with initial conditions $v_0 \in V$, the exponential map is:

$$\exp_{Id} : v_0 \in V \mapsto \rho_{v_0}(1) \in \Phi \quad \text{and} \quad d_\Phi^2(Id, \exp_{Id}(v_0)) = \|v_0\|_V^2$$

[1]. Beg, M. F., Miller, M. I., Trouné, A., and Younes, L. Computing large deformation metric mappings via geodesic flows of diffeomorphisms.

[2] Miller, M. I., Trouné, A., and Younes, L.. Geodesic shooting for computational anatomy.

I. Computing the Exponential map [1]

Let denote $K : \mathbb{R}^n \times \mathbb{R}^n \rightarrow \mathbb{R}^{n^2}$ the kernel of the RKHS \mathcal{V} .

Given N_0 control points $\mathbf{X}_0 = (x_k^0)_{k \in [N_0]} \in (\mathbb{R}^n)^{N_0}$, and momentums $\alpha = (\alpha_k^0)_{k \in [N_0]} \in (\mathbb{R}^n)^{N_0}$, the initial velocity field is,

$$v_0 : x \in \mathbb{R}^n \mapsto \sum_{i \in [N_0]} K(x_k^0, x) \alpha_k^0 \in \mathbb{R}^n .$$

Then, for any $\tau \in [0, 1]$,

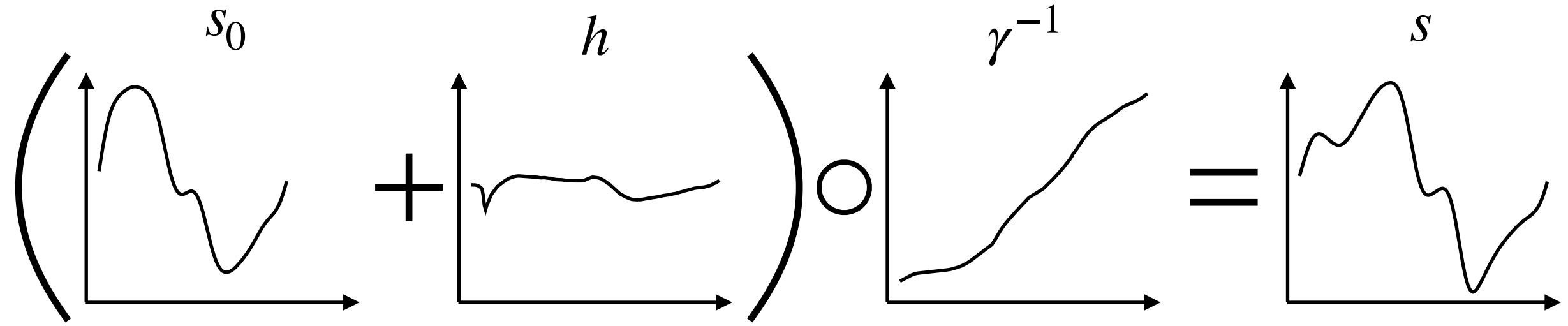
$$v_\tau : x \in \mathbb{R}^n \mapsto \sum_{i \in [N_0]} K(x_k(\tau), x) \alpha_k(\tau) \in \mathbb{R}^n ,$$

governed by the geodesic equations:

$$(E) \quad \begin{cases} \frac{dx_k(\tau)}{d\tau} = v_\tau(x_k(\tau)) \\ \frac{d\alpha_k(\tau)}{d\tau} = - \sum_{l \in N_0} d_{x_k(\tau)} K(x_k(\tau), x_l(\tau)) \alpha_l(\tau)^\top \alpha_k(\tau) \end{cases} \quad \text{with } \forall k \in [N_0] \quad \begin{cases} x_k(0) = x_k^0 \\ \alpha_k(0) = \alpha_k^0 \end{cases}$$

II. Time series deformation representation

Intuition. Let $s_0 : \mathbf{I} \mapsto \mathbb{R}^d$ and $s : \mathbf{J} \mapsto \mathbb{R}^d$, the diffeomorphic deformation ϕ mapping s_0 to s should be seen as distortion $h : \mathbf{I} \mapsto \mathbb{R}^d$ and a time parametrization $\gamma^{-1} : \mathbf{J} \mapsto \mathbf{I}$ such that: $\phi \cdot \mathbf{G}(s_0) = \mathbf{G}((s_0 + h) \circ \gamma^{-1}) = \mathbf{G}(s)$



Theorem. For any continuously differentiable time series $s_0 : \mathbf{I} \mapsto \mathbb{R}^d$ and $s : \mathbf{J} \mapsto \mathbb{R}^d$, there exists deformations $\Psi_\gamma : (t, x) \in \mathbb{R}^{d+1} \mapsto (\gamma(t), x) \in \mathbb{R}^{d+1}$ with $\gamma \in \mathbf{D}(\mathbb{R})$, and $\Pi_f : (t, x) \in \mathbb{R}^{d+1} \mapsto (t, f(t, x)) \in \mathbb{R}^{d+1}$ with $f \in \mathbf{C}^1(\mathbb{R}^{d+1}, \mathbb{R}^d)$, such that:

$$\phi_{\gamma, f} \cdot \mathbf{G}(s_0) = \mathbf{G}(s) \quad \text{with} \quad \phi_{\gamma, f} = \Psi_\gamma \circ \Pi_f,$$

Moreover, for any $\bar{\gamma} \in \mathbf{D}(\mathbb{R})$, and $\bar{f} \in \mathbf{C}^1(\mathbb{R}^{d+1}, \mathbb{R}^d)$, $\phi_{\bar{\gamma}, \bar{f}} \cdot \mathbf{G}(s_0)$ is the graph of a continuously differentiable time series.

Remark. For any time series $s_0 : \mathbf{I} \mapsto \mathbb{R}^d$ and deformation $\phi_{\bar{\gamma}, \bar{f}}$, the time parametrization and the distortion are:

$$\begin{cases} \gamma^{-1} : t \in \bar{\gamma}(\mathbf{I}) \mapsto \bar{\gamma}^{-1}(t) \in \mathbf{I} \\ h : t \in \mathbf{I} \mapsto \bar{f}(t, s_0(t)) - s_0(t) \end{cases}$$

II. A kernel for time series deformations

Gaussian kernel. For any $n \in \mathbb{N}^*$ and $\sigma > 0$, the one-dimensional Gaussian kernel is defined as,

$$K_\sigma^{(n)} : (x, y) \in \mathbb{R}^b \times \mathbb{R}^n \mapsto \exp(-\|x - y\|^2/\sigma).$$

The proposed kernel. We consider the kernel K_G defined for any $(t, x), (t', x') \in (\mathbb{R}^{d+1})^2$,

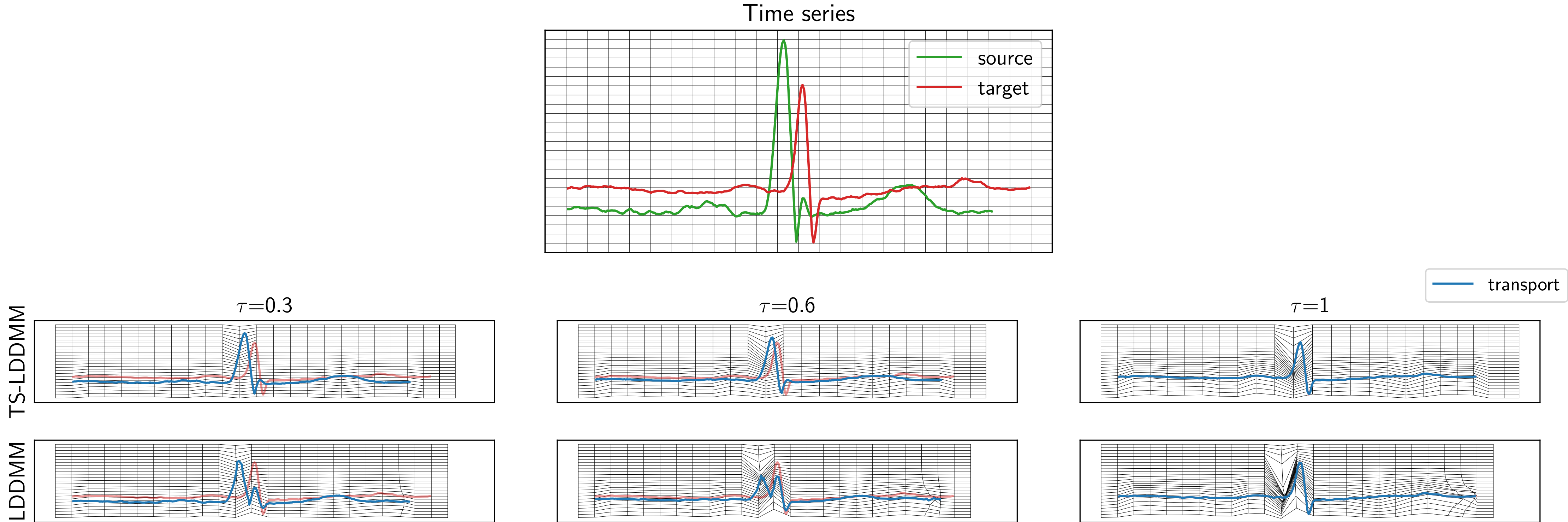
$$K_G((t, x), (t', x')) = \begin{pmatrix} c_0 K_{\text{time}} & 0 \\ 0 & c_1 K_{\text{space}} \end{pmatrix} \quad \text{with} \quad \begin{cases} K_{\text{time}} = K_{\sigma_{T,0}}^{(1)}(t, t') \\ K_{\text{space}} = K_{\sigma_{T,1}}^{(1)}(t, t') K_{\sigma_x}^{(d)}(x, x') I_d \end{cases}$$

parametrized by $\sigma_{T,0}, \sigma_{T,1}, \sigma_x > 0$ and the constants $c_0, c_1 > 0$.

Lemma. For any initial velocity field $v_0 \in V$, the RKHS associated to K_G , the diffeomorphic deformations learned by geodesic shooting ensures a time series graph structure along its geodesic path, i.e.

For any $\tau \in [0, 1]$, there exist $\gamma_\tau \in D(\mathbb{R})$ and $f_\tau \in C^1(\mathbb{R}^{d+1}, \mathbb{R}^d)$ such that $\exp_{Id}(\tau v_0) = \Psi_{\gamma_\tau} \circ \Pi_{f_\tau}$.

II. Difference between LDDMM and TS-LDDMM



- Large Deformation Diffeomorphic Metric Mapping (LDDMM) with a RBF kernel
- TS-LDDMM an adaptation of LDDMM to time series (our contributions).

III. The varifold distance between time series graph [1]

Let $\mathbf{G} = (g_j)_{j \in [T]} \in (\mathbb{R}^{d+1})^T$ be a sampled time series graph. The approximate varifold representation of \mathbf{G} is the measure,

$$\mu_{\mathbf{G}} = \sum_{j \in [T-1]} l_j \delta_{(x_j, \vec{v}_j)} \quad \text{with} \quad \begin{cases} l_j = \|g_{j+1} - g_j\| \\ x_j = (g_j + g_{j+1})/2 \\ \vec{v}_j = (g_{j+1} - g_j)/\|g_{j+1} - g_j\| \end{cases}$$

Assuming that test functions belong to the dual of an RKHS \mathbf{W} with kernel $k = k_{pos} \otimes k_{dir} : \mathbb{R}^{d+1} \times \mathbb{S}^d \mapsto \mathbb{R}$, such that,

$$\langle \delta_{(x_1, \vec{v}_1)}, \delta_{(x_2, \vec{v}_2)} \rangle_{\mathbf{W}^*} = k_{pos}(x_1, x_2) k_{dir}(\vec{v}_1, \vec{v}_2).$$

The similarity between time series graphs $\mathbf{G}_1 = (g_j^1)_{j \in [T_1]}$ and $\mathbf{G}_2 = (g_j^2)_{j \in [T_2]}$ is given by,

$$d_{\mathbf{G}}^2(\mathbf{G}_1, \mathbf{G}_2) = \|\mu_{\mathbf{G}_1} - \mu_{\mathbf{G}_2}\|_{\mathbf{W}^*}^2 = \langle \mu_{\mathbf{G}_1}, \mu_{\mathbf{G}_1} \rangle_{\mathbf{W}^*} - 2\langle \mu_{\mathbf{G}_1}, \mu_{\mathbf{G}_2} \rangle_{\mathbf{W}^*} + \langle \mu_{\mathbf{G}_2}, \mu_{\mathbf{G}_2} \rangle_{\mathbf{W}^*}$$

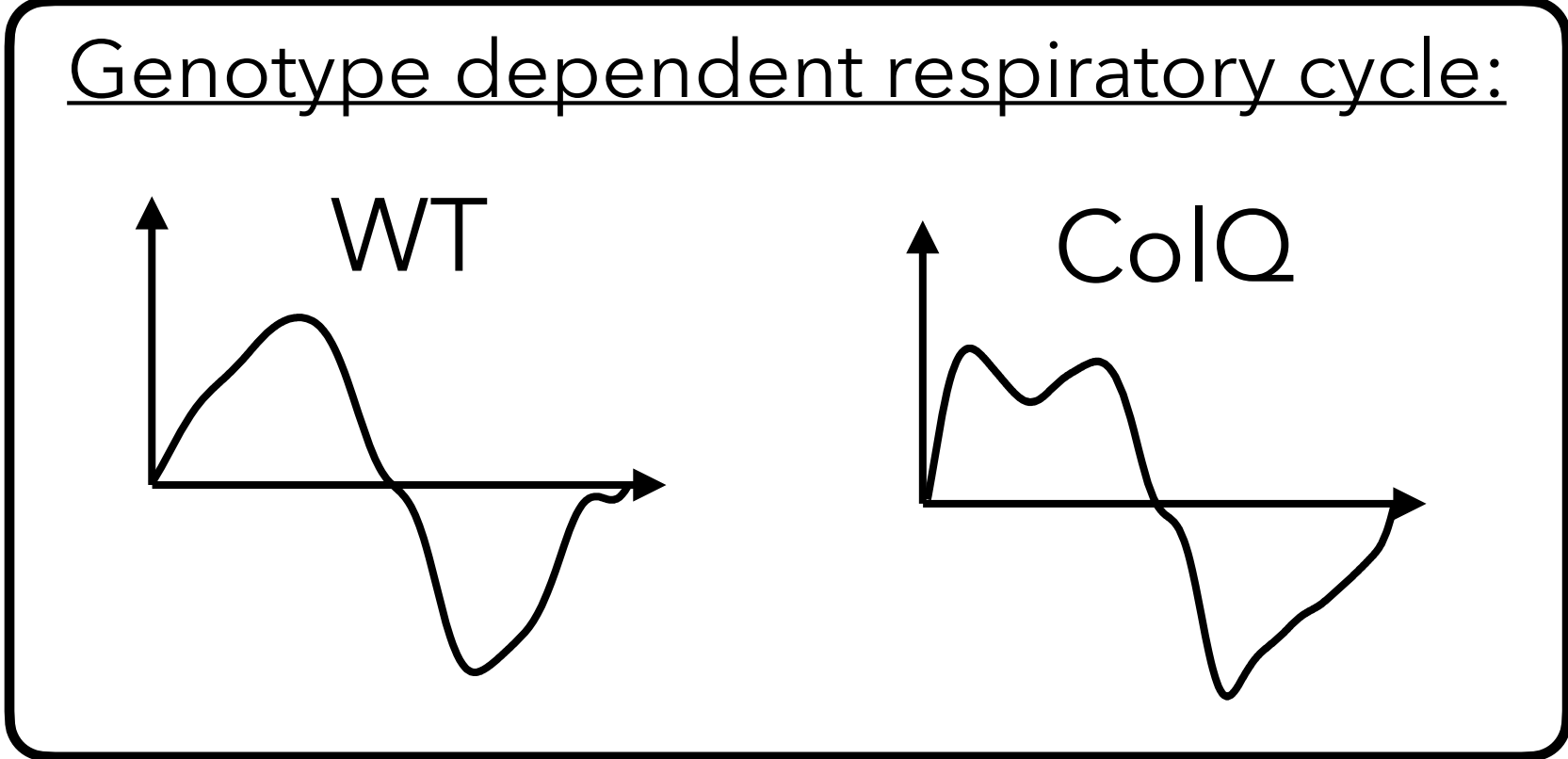
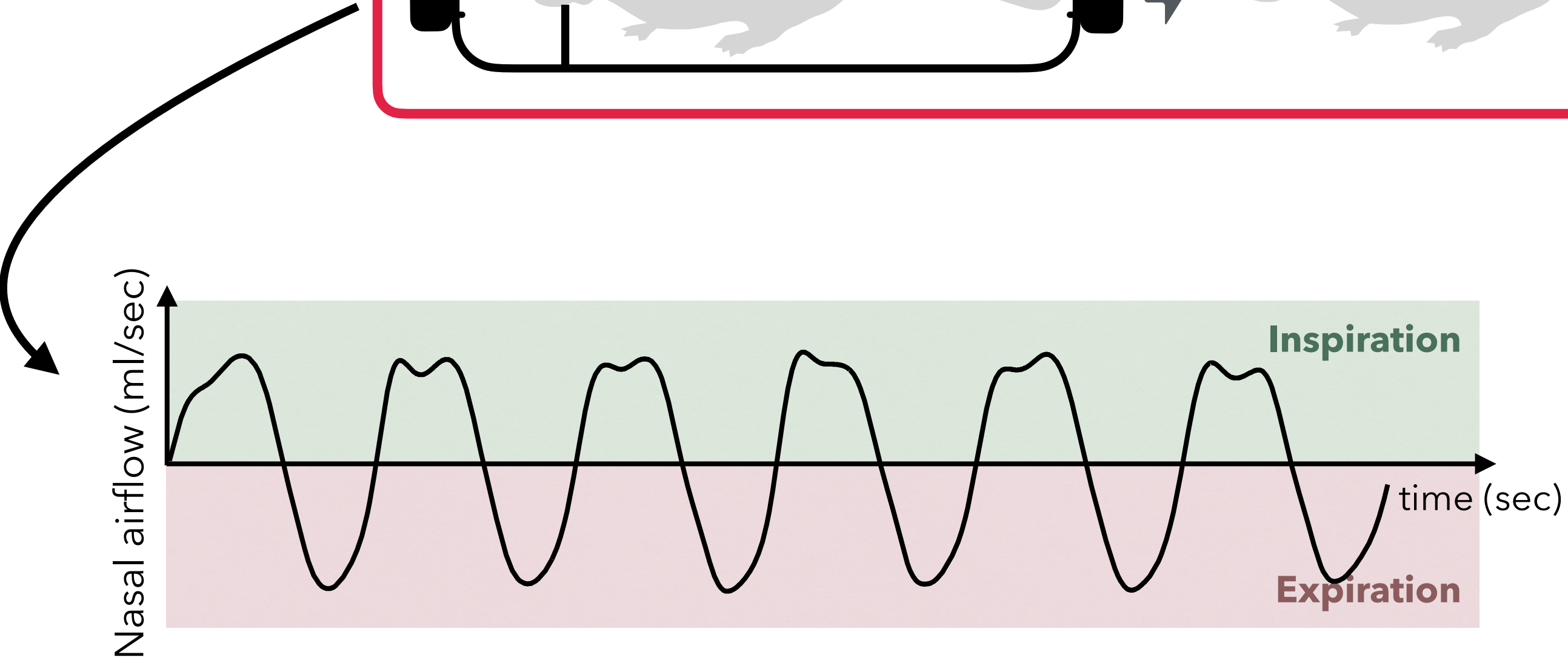
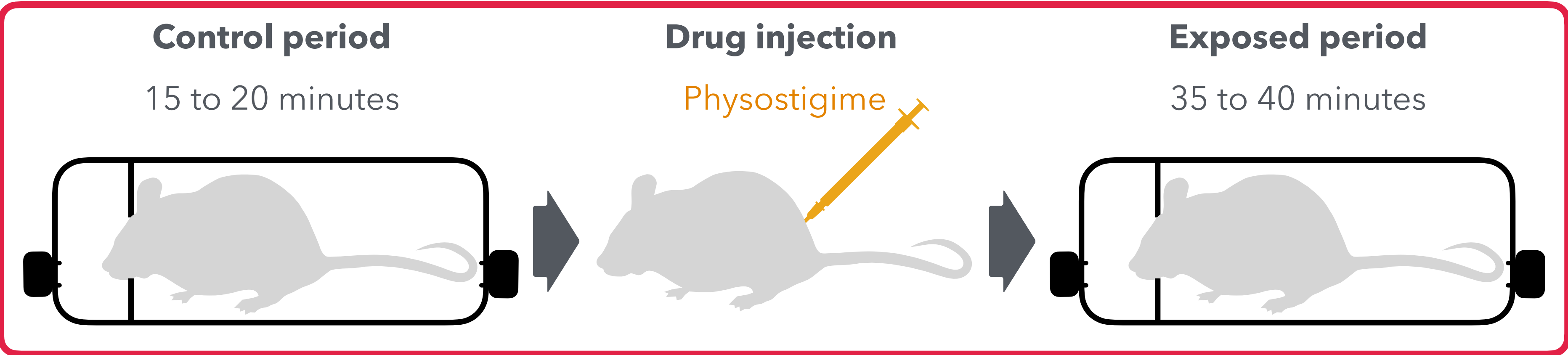
with,

$$\langle \mu_{\mathbf{G}_1}, \mu_{\mathbf{G}_2} \rangle_{\mathbf{W}^*} = \sum_{i \in [T_1-1]} \sum_{j \in [T_2-1]} l_i^1 l_j^2 k_{pos}(x_i^1, x_j^2) k_{dir}(\vec{v}_i^1, \vec{v}_j^2)$$

Further experiments

Mice ventilation analysis before/after drug injection

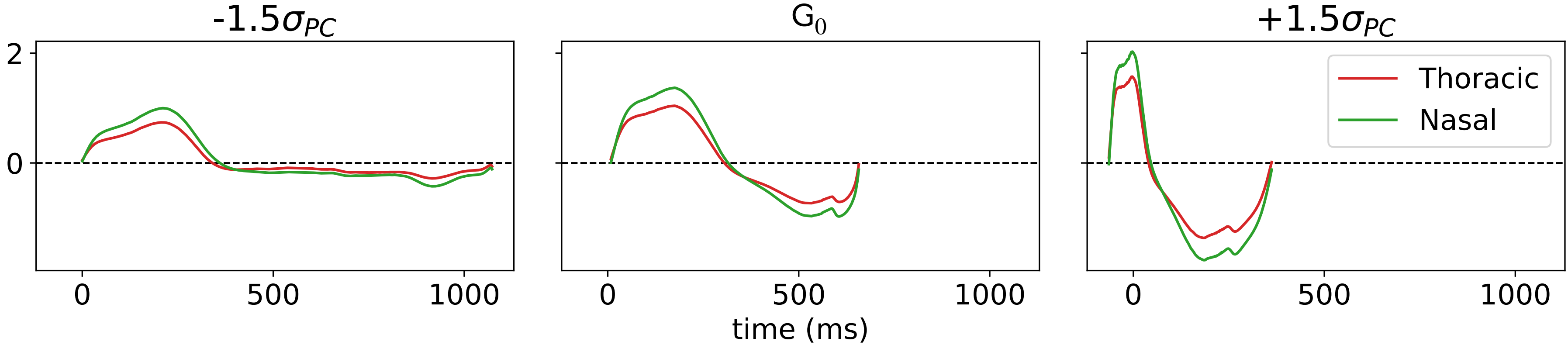
For mice of different genotype (ColQ or WT):



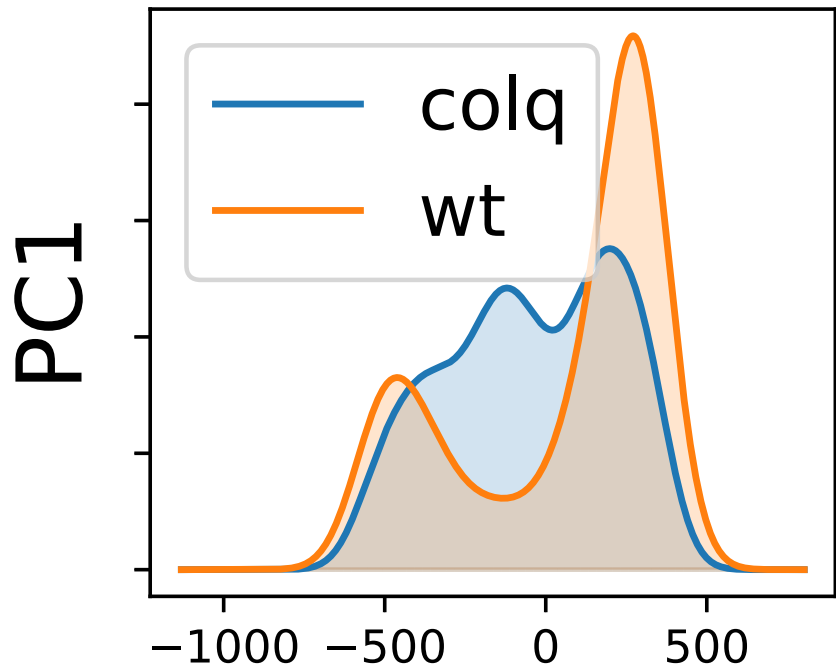
Mice ventilation analysis before/after drug injection

Kernel PCA is applied on the initial velocity field parameters $(G_0, \alpha_i)_{i \in [N]}$, resulting in the K principal axis of deformations with the initial velocity field $(G_0, \alpha_j^{pc})_{j \in [K]}$.

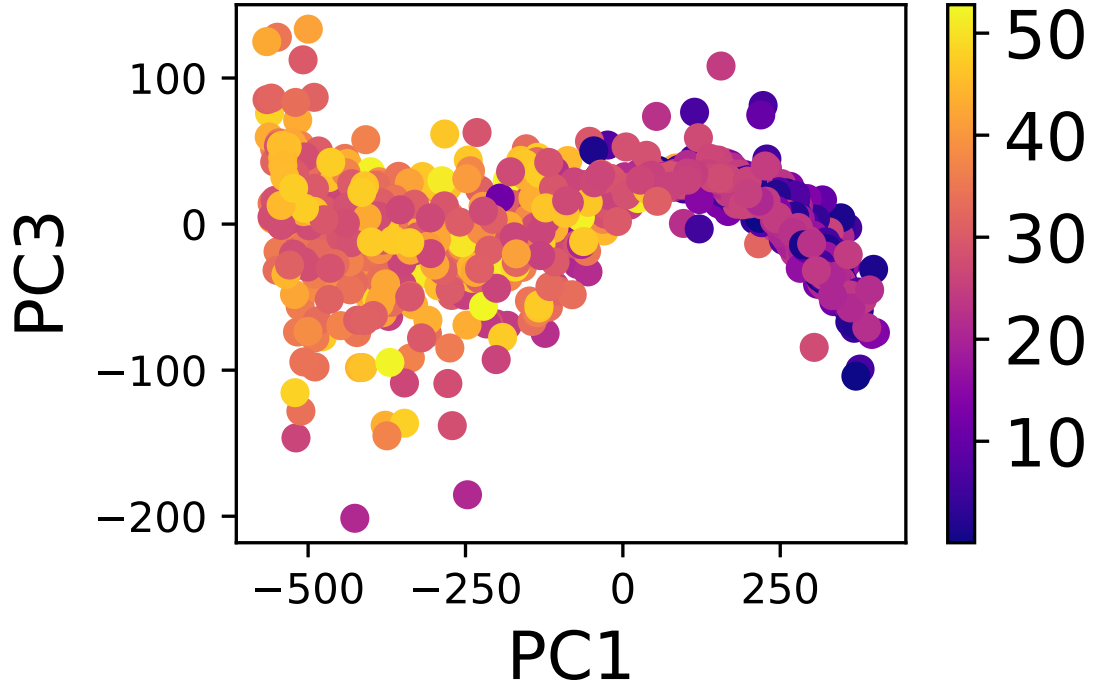
(a) TS-LDDMM PC1 shooting



(b) PC1 densities



(c) Scatter PC1 vs PC3



Benchmark on classification task on 15 UCR/UEA datasets:

Robustness to irregular sampling, comparison with state-of-the-art in deep learning.

Comparison of average f1 score (macro) and ranks as the sample dropping rate increases. **First** & second best performers. TS-LDDMM is the best performer on three out of four dropping rates.

| Methods | Regular | | 30 % dropped | | 50 % dropped | | 70 % dropped | |
|---------------------|--------------------|-------------|-------------------|-------------|--------------------|-------------|--------------------|-------------|
| | F1-score | Rank | F1-score | Rank | F1-score | Rank | F1-score | Rank |
| RNN (1999) | 0.64 ± 0.21 | 6.2 | 0.53 ± 0.23 | 6.6 | 0.48 ± 0.21 | 7.2 | 0.44 ± 0.21 | 6.07 |
| LSTM (1997) | 0.61 ± 0.29 | 6.0 | 0.57 ± 0.29 | 6.27 | 0.53 ± 0.25 | 6.07 | 0.51 ± 0.29 | 5.27 |
| GRU (2014) | 0.71 ± 0.26 | 4.2 | 0.68 ± 0.28 | 4.27 | 0.66 ± 0.28 | 3.73 | <u>0.59 ± 0.28</u> | <u>3.67</u> |
| MTAN (2021) | 0.59 ± 0.28 | 7.13 | 0.58 ± 0.28 | 5.8 | 0.54 ± 0.29 | 5.33 | 0.51 ± 0.28 | 5.0 |
| MIAM (2022) | 0.48 ± 0.35 | 6.93 | 0.42 ± 0.33 | 8.27 | 0.47 ± 0.31 | 6.93 | 0.35 ± 0.31 | 7.6 |
| ODE-LSTM (2020) | 0.63 ± 0.24 | 6.0 | 0.57 ± 0.25 | 6.53 | 0.51 ± 0.24 | 7.27 | 0.45 ± 0.23 | 6.73 |
| Neural SDE (2019) | 0.48 ± 0.28 | 7.67 | 0.47 ± 0.26 | 7.47 | 0.45 ± 0.27 | 7.13 | 0.45 ± 0.25 | 6.0 |
| Neural LNSDE (2024) | 0.7 ± 0.27 | <u>3.87</u> | 0.68 ± 0.29 | <u>4.0</u> | <u>0.67 ± 0.25</u> | <u>3.53</u> | 0.66 ± 0.23 | 2.47 |
| LDDMM (2008) | <u>0.72 ± 0.2</u> | 4.53 | <u>0.7 ± 0.21</u> | 4.2 | 0.57 ± 0.25 | 5.0 | 0.4 ± 0.25 | 7.13 |
| TS-LDDMM (ours) | 0.83 ± 0.18 | 2.93 | 0.8 ± 0.18 | 2.07 | 0.7 ± 0.26 | 3.33 | 0.51 ± 0.27 | 5.67 |

Benchmark on classification task on 15 UCR/UEA datasets

Regular sampling, comparison with state-of-the-art in Functional Data Analysis.

Comparison of average f1 score (macro) between methods from shape analysis and functional data analysis.
First & second best performers.

| | Dataset | Shape-FPCA (2024) | TCLR (2024) | LDDMM (2008) | TS-LDDMM (ours) |
|--------------|---------------------------|-------------------|-------------|--------------|-----------------|
| Univariate | ArrowHead | 0.18 | 0.75 | 0.84 | 0.91 |
| | BME | 0.16 | 1.00 | 0.82 | 1.00 |
| | ECG200 | 0.40 | 0.67 | 0.81 | 0.79 |
| | FacesUCR | 0.08 | 0.73 | 0.69 | 0.86 |
| | GunPoint | 0.93 | 0.97 | 0.83 | 1.00 |
| | PhalangesOutlinesCorrect | 0.39 | 0.63 | 0.53 | 0.52 |
| | Trace | 0.55 | 1.00 | 0.46 | 1.00 |
| Multivariate | ArticularyWordRecognition | — | — | 0.98 | 1.00 |
| | Cricket | — | — | 0.77 | 0.93 |
| | ERing | — | — | 0.95 | 0.98 |
| | Handwriting | — | — | 0.22 | 0.44 |
| | Libras | — | — | 0.56 | 0.60 |
| | NATOPS | — | — | 0.82 | 0.82 |
| | RacketSports | — | — | 0.83 | 0.79 |
| | UWaveGestureLibrary | — | — | 0.72 | 0.81 |